How to cite: *Angew. Chem. Int. Ed.* **2021**, *60*, 25674–25679
International Edition: doi.org/10.1002/anie.202108242
German Edition: doi.org/10.1002/ange.202108242

Proton Transfer | Hot Paper

Double Proton Transfer Across a Table: The Formic Acid Dimer–Fluorobenzene Complex

Weixing Li, Denis S. Tikhonov, and Melanie Schnell**

Abstract: *Proton transfer via tunneling is a fundamental quantum-mechanical phenomenon. We report rotational spectroscopy measurements of this process in the complex of the formic acid dimer with fluorobenzene. The assignment of the spectrum indicates that this complex exists in the form of a π–π stacked structure. Each rotational transition of the parent isotopologue exhibits splitting. Isotopic substitution experiments show that the spectral splitting results from double-proton transfer tunneling in the formic acid dimer. Presence of fluorobenzene as a neighboring molecule does not quench the double proton transfer in the formic acid dimer but decreases its tunneling splitting from 341(3) MHz to 267.608(1) MHz. Calculations suggest that the presence of the weakly bounded fluorobenzene does not influence the activation energy of the proton transfer. The fluorobenzene is reoriented with respect to the formic acid dimer during the course of the reaction, slowing down the proton transfer motion.*

Intermolecular proton transfer along hydrogen bonds is a fundamental and ubiquitous reaction in many biological and chemical systems, and the dynamics of those reactions is being strongly governed by the tunneling effect.[1–5] Proton transfer proceeds as an exchange of hydrogen between the acid (AH) and the base (B) via the chemical reaction[6,7] A–H···B⇌A···H–B that is also an elementary step in the Grotthuss mechanism.[8] In the symmetric cases (when A is identical to B), tunneling manifests itself through splitting the A-H vibrational states of the system. This reaction depends not only on the acid-base pair involved but also on the neighboring environment.[9] Thus, an accurate description of proton tunneling influenced by nearby molecules is important for understanding many chemical processes, including biochemical ones.[5,9] From the theoretical view, the subtle interplay of the partner molecules has significant influence on proton tunneling.[10–13] Previous experimental studies have shown that the surrounding environment can modify the proton transfer rate,[14–19] however, little experimental data is available on how the proton tunneling process is affected by the environment at the few-molecules level. Herein, we report the direct observation and precise measurement of proton transfer of the formic acid dimer lying on the surface of an aromatic π system. The results reveal that the neighboring molecule decreases the rate of the proton transfer tunneling process.

For a molecular cluster, in general, different configurations are distinguishable and acquire different energies. In asymmetric environments, the delocalization of the protons by tunneling usually competes with the localization of the protons by the environment, and the latter usually wins, with only a few exceptions reported so far.[20] As a result, it is rare to observe proton tunneling in molecular complexes. Yet, the observation of tunneling is possible in cases where the configurations undergo symmetric conversion. For the complex of fluorobenzene (PhF)–formic acid dimer (FAD), the most stable configuration adopts a π–π stacked structure (see Figure 1),[21] which allows to retain the permutation–inversion symmetry along the double proton transfer path.

In this study, we utilize chirped-pulse Fourier transform microwave (CP-FTMW) spectroscopy in the 2–8 GHz frequency range to measure the pure rotational spectra of the PhF-FAD cluster and perform quantum-chemical modeling to calculate proton transfer properties. Microwave spectros-

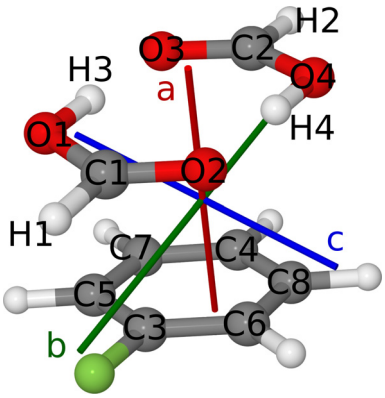

Figure 1. The configuration of the PhF-FAD cluster with atom numbering and principal axes system.

[*] Dr. W. Li, Dr. D. S. Tikhonov, Prof. Dr. M. Schnell
Deutsches Elektronen-Synchrotron DESY
Notkestr. 85, 22607 Hamburg (Germany)
E-mail: melanie.schnell@desy.de
Dr. W. Li, Dr. D. S. Tikhonov, Prof. Dr. M. Schnell
Institute of Physical Chemistry
Christian-Albrechts-Universität zu Kiel
Max-Eyth-Str. 1, 24118 Kiel (Germany)
Dr. W. Li
Current address: Department of Chemistry, Fudan University
Songhu Rd. 2005, 200438 Shanghai (China)
E-mail: weixingli@fudan.edu.cn
Supporting information and the ORCID identification number(s) for the author(s) of this article can be found under: https://doi.org/10.1002/anie.202108242.

copy is a well-established experimental technique for the study of large-amplitude motions (LAM) in molecules.[22] These low frequency vibrations couple with the overall molecular rotation leading to splitting of rotational energy levels. Therefore, information about the LAM is encoded in the rotational spectra. Besides the parent species, isotope effects associated with proton tunneling in this complex have also been investigated, providing unambiguous evidence for the double proton transfer being the source of the splitting in rotational spectra.

In the rotational spectra of PhF-FAD, the transitions exhibit a splitting pattern as depicted in the upper part of Figure 2. Each transition splits into two components due to tunneling, and in total 460 transition frequencies within 2–8 GHz have been assigned to two LAM vibrational states 0^+ and 0^- (symmetric and antisymmetric along the LAM coordinate, respectively). The fitted spectroscopic constants for these two sub-states of the complex are reported in Table 1.

Table 1: Experimental and theoretical rotational parameters of PhF-FAD complex.

	Experiment[a]		Theory		
	Parent(0^+)	Parent(0^-)	B3LYP-D3BJ[b]	B2PLYP[b]	PBEh-3c
A [MHz]	902.68022(20)	902.67985(22)	903.6	900.1	915.0
B [MHz]	700.65306(20)	700.64869(19)	704.4	655.0	721.9
C [MHz]	539.71027(21)	539.70937(20)	534.0	509.2	553.1
D_J [kHz]	0.3434(14)				
D_{JK} [kHz]	0.5467(13)				
D_K [kHz]	−0.2474(14)				
d_1 [kHz]	−0.08985(18)				
d_2 [kHz]	0.024958(60)				
ΔE_{01} [MHz]	267.6080(13)				
F_{bc} [MHz]	15.57228(16)				
F_{ca} [MHz]	17.3378(17)				
$\mu_a/\mu_b/\mu_c$ [D]	intra-/intra-/inter-[c]		0.9/1.2/0.2	1.0/1.2/0.1	1.0/1.1/0.1
σ[d][kHz]	5.358				
N[e]	460				

[a] Standard deviations within parentheses are expressed in units of the last two digits. [b] Calculated using the def2-TZVP basis set and geometrical counterpoise (gCP) correction. [c] intra- denotes intra-state transition; inter- denotes inter-state transition. [d] Root-mean-square deviation of the fit. [e] Number of the lines in the fit.

By accumulating 19.6 million free induction decay (FID) signals, the high signal-to-noise ratio of the spectrum allows us to assign the ^{13}C mono-substituted isotopologues in natural abundance. A portion of the spectrum including all singly-substituted ^{13}C isotopologues is shown in the lower part of Figure 2. As one can see, the isotopologues with $^{13}C1$, $^{13}C2$,

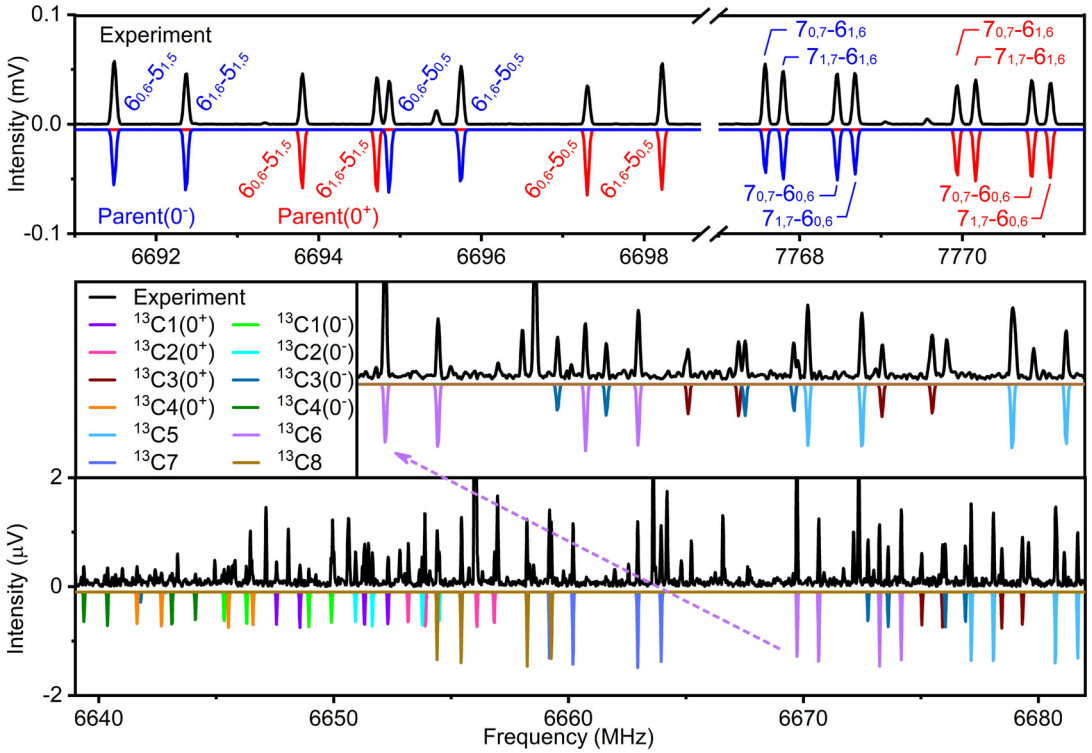

Figure 2. Parts of the rotational spectra of the parent species (upper) and mono-substituted ^{13}C isotopologues (lower). The black traces represent the experimental spectra while the colored traces are simulated spectra based on the fitted spectroscopic parameters of the respective isotopologues. The quantum numbers are defined using the standard nomenclature for the rotational energy levels of an asymmetric top, denoted as J_{K_a,K_c}, where J is the quantum number for the total rotational angular momentum, and K_a and K_c are the quantum numbers for the projection of total rotational angular momentum onto the symmetry axes (a and c) in the two limiting cases of prolate and oblate symmetric tops, respectively. Lower: only the $J_{upper} = 6$ rotational transitions of ^{13}C substituted species are shown. The experimental lines without simulated counterparts might arise from other molecular species in the molecular beam, such as complexes with water or with the carrier gas.

^{13}C3, and ^{13}C4 substitution display a similar splitting pattern as the parent species, whereas the other four isotopologues do not show any splitting pattern. The spectral intensities of the latter case are around twice as strong as for the former, because the tunneling splitting divides the population into the two sub-states. The transition frequencies and fitted spectroscopic parameters are listed in the supplementary materials.

Tunneling in clusters usually can occur when the molecules within the cluster rearrange to produce an equivalent structure.[23] In this complex, double proton transfer in the FAD moiety is the only motion linked by short and energetically accessible pathways to produce an observable tunneling splitting. The spectra of the isotopologues, whose isotopic substitution is near the *ab* plane (^{13}C1, ^{13}C2, ^{13}C3, ^{13}C4), show the characteristic splitting pattern as observed for the parent species, while the spectra of the isotopologues with isotopic substitution far from the *ab* plane (^{13}C5, ^{13}C6, ^{13}C7, ^{13}C8) have no splitting pattern. This, together with the interstate transitions being of *c*-type, strongly points to proton transfer in FAD being the source of the splitting in PhF-FAD. During the proton transfer process, the permutation-inversion symmetry of the complex is kept upon isotopic substitution of the atoms close to the *ab* plane, whereas the symmetry is reduced by ^{13}C single substitutions far from the *ab* plane, quenching the tunneling. The tunneling splitting of the complex has been determined to be 267.6080(13) MHz, which is much smaller than that of FAD (341(3) MHz).[24,25] This result could be intuitively expected since quantum tunneling splitting is associated with the potential barrier height and width, and the interactions between PhF and the protons of FAD could obstruct or guide the exchange of the protons.

To explain how the presence of the PhF molecule affects the proton tunneling motion in FAD, we have performed theoretical calculations for PhF-FAD and for the FAD as a comparison. The potential energy surfaces (PES) for double proton transfer in FAD and PhF-FAD were computed at PBEh-3c and DFT/def2-TZVP (with DFT = B1LYP, B3LYP, mPW1LYP and X3LYP) levels of theory. The reaction coordinate scans were performed by simultaneously changing the O1-H3 and O4-H4 distances (r(O1H3) and r(O4H4), respectively). Owing to complicated and weak interactions guiding the relative arrangement of the PhF and FAD, the standard DFT-D3BJ approach failed to produce a smooth potential scan and the symmetric transition state for the proton transfer reaction: the orientation of FAD with respect to PhF in the vicinity of the transition state turned out to be hard to capture, it leads to a non-symmetric transition state for the proton transfer. Only PBEh-3c behaved robust enough in these calculations. To perform the DFT/def2-TZVP simulation of double proton transfer in the PhF-FAD complex, we have applied a QM/MM approach, where we parameterized the symmetry adapted perturbation theory (SAPT) interaction energy at the SAPT2/aug-cc-pVDZ level between PhF and FAD in the MM potential (see SI for details). The SAPT calculations revealed that the FAD interaction with PhF is mainly governed by attractive dispersion and repulsive exchange interactions with little contribution from electrostatics and almost none from induction (see Figure 3). Interestingly, due to the planarity of the FAD and PhF moieties and the π–π stacked structure, the dissociation energy of PhF from FAD (22 kJ mol^{-1} at the SAPT2/aug-cc-pVTZ//PBEh-3c level of theory) is only three times lower than the dissociation energy of FAD itself (59.5(5) kJ mol^{-1}[26]).

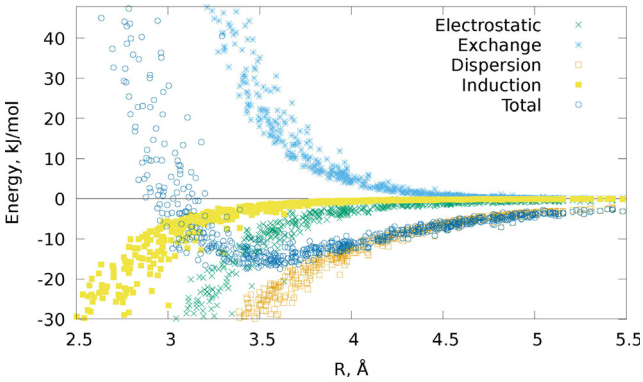

Figure 3. SAPT2/aug-cc-pVTZ interaction energies of FAD with PhF. *R* denotes the distance between the FAD and PhF centers of mass.

The proton transfer dynamics was computed in the framework of an effective one-dimensional Schrödinger equation (SI) with the reaction coordinate [Eq. (1)]:

$$\xi = (r(\mathrm{O1H3}) + r(\mathrm{O4H4}) - r(\mathrm{O3H3}) - r(\mathrm{O2H4}))/\sqrt{8} \quad (1)$$

The resulting splittings along with the barrier heights and effective barrier heights (including zero-point vibrational corrections for the other degrees of freedom) are given in Table 2.

The simulation based on the PBEh-3c calculations shows an astonishing match with the experimental data for both FAD and PhF-FAD. Amongst the hybrid DFT with def2-TZVP basis set, the best agreement show B1LYP and mPW1LYP functionals, while B3LYP and X3LYP slightly lower the barrier for intermolecular proton transfer and thus lead to larger tunneling splittings. Nevertheless, all the theoretical estimations are in a reasonable agreement with the experimental data. The barrier heights for the reaction are

Table 2: Experimental and theoretical proton transfer tunneling splittings (ΔE_{01}), barrier heights (E_{BH}), and effective barrier heights (E_{BH}^{eff}) in FAD and in the PhF-FAD cluster.

Quantity	Molecule	Experiment	PBEh-3c	DFT/def2-TZVP			
				B1LYP	B3LYP	mPW1LYP	X3LYP
ΔE_{01} [MHz]	FAD	341(3)	359	182	1857	465	2564
	PhF-FAD	267.6080(13)	269[a]/89	136[a]	752[a]	281[a]	1405[a]
E_{BH} [cm^{-1}]	FAD		2170	2395	2127	2324	2108
	PhF-FAD		2119[a]/2123	2371[a]	2104[a]	2300[a]	2085[a]
E_{BH}^{eff} [cm^{-1}]	FAD		630	914	708	820	691
	PhF-FAD		656[a]/757	911[a]	769[a]	894[a]	739[a]

[a] Value obtained from QM/MM calculations.

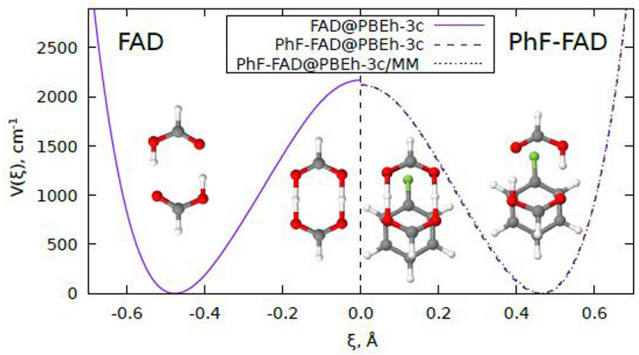

Figure 4. Theoretical potential energy surfaces for proton transfer in FAD and PhF-FAD. ξ denotes the proton transfer coordinate [Eq. (1)].

surprisingly similar for PhF-FAD and for FAD, which indicates that the PhF has no significant influence on the PES of FAD (see also Figure 4).

The main difference between double proton transfer in FAD and in PhF-FAD is the reorientation of FAD with respect to PhF during the course of the reaction, with the most prominent change being the internal counter rotation of FAD and PhF around the *a*-axis of the complex (see Figure 1). Therefore, a natural explanation of the observed lowering of the tunneling splitting in PhF-FAD with respect to FAD is the Marcus charge transfer theory[27] applied to proton transfer reactions.[28–31] Let us assume that the proton transfer motion is linearly coupled with an environment (PhF) small-amplitude motion with a frequency of ν. If we freeze the rearrangement of PhF with respect to FAD, we would observe an energy difference between two minima λ_e (see Figure 5), and this energy can be called the reorganization energy. By applying second-order perturbation theory (see SI for more details), we can obtain the following relation between tunneling splittings in the free FAD (ΔE_{free}) and in the FAD with the environment (ΔE_{env}):

$$\Delta E_{env} = \Delta E_{free}\left(1 - \frac{\lambda_e}{2h\nu}\right)$$

Since $\frac{\lambda_e}{2h\nu} \geq 0$, the reorganization model suggests that an additional coupled motion should decrease the tunneling rate, which agrees with the experimentally and computationally observed results. We can imagine PhF acting as a heavy backpack in the double proton transfer: by adding more atoms to be moved during the reaction, it lowers the tunneling rate in the PhF-FAD complex with respect to pure FAD. This metaphor can be visualized through the plots of the coordinate-dependent mass of the proton transfer motions (SI).

For the ^{13}C isotopologues in natural abundance, we fixed the tunneling splitting values to that of the parent species when we fit their spectra to the rotational Hamiltonian. Therefore, we did not observe any information of how ^{13}C substitutions influences the tunneling process. To examine the isotopologue effect on the tunneling splitting, we measured the spectra of PhF-$(DCOOH)_2$, PhF-(DCOOH)-(HCOOH), and PhF-(HCOOH)-(DCOOH). As shown in Figure 6a,b, the spectra of all three species show the splitting pattern. By fitting ca. 160 transitions for each isotopic species, we obtained tunneling splittings of 275.7992(84), 274.0545(77), and 269.2596(74) MHz for D1D2, D1H2, and H1D2, respectively, somewhat larger than that of the parent species (267.6080(13) MHz). As a comparison, the tunneling splitting of mono-deuterated FAD was determined to be 331.6(5) MHz.[24] The theoretical tunneling frequency of this isotopologue computed at PBEh-3c was found to be 178 MHz. The relatively large deviation from the experiment is probably caused by a reduced performance of the applied method in the cases of the isotopologues due to vibrational non-adiabatic effects.[32]

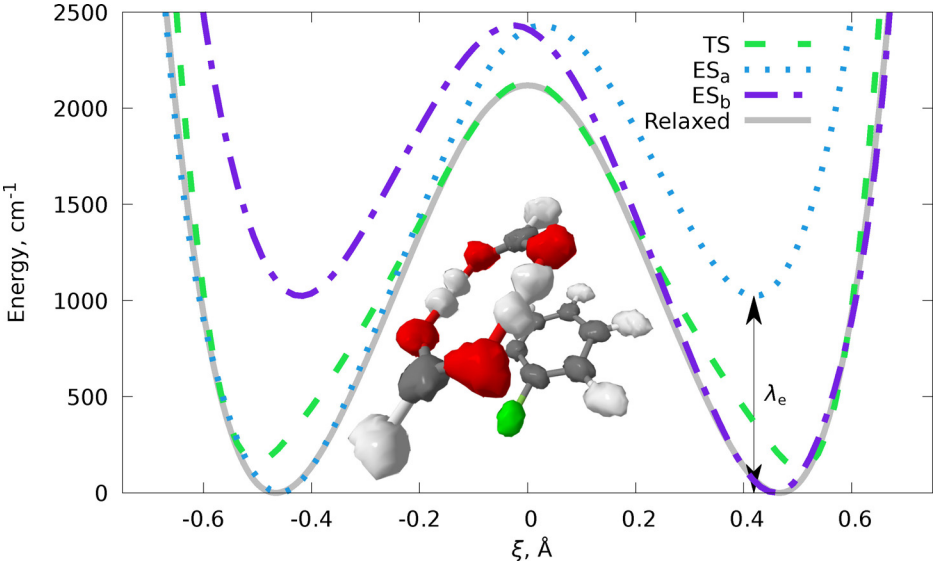

Figure 5. Theoretical potential energy surfaces for proton transfer in the PhF-FAD complex at three different orientations of FAD with respect to the PhF frame. ES_a and ES_b denote the orientation frozen at the two possible equilibrium structures, TS is the orientation frozen at the reaction transition state, "Relaxed" denotes fully relaxed scan (corresponds to the data shown in Figure 4), ξ is the proton transfer coordinate (Equation 1). The averaged vibrational ground state structure of PhF-FAD at the PBEh-3c level of theory is also shown. All the curves were obtained at the PBEh-3c/MM level of theory.

To further elucidate the tunneling motion, we performed another measurement by replacing formic acid (HCOOH) with HCOOD. HCOOD was obtained by mixing formic acid with D_2O. A section of the spectrum is shown, which does not exhibit any splittings (Figure 6(c)), independent if one or two deuterium atoms are incorporated into FAD. This result confirms the attribution of the splitting to the concerted proton tunneling motion. The deuteration of a single -OH group (H3D4 and D3H4) breaks down the symmetry of the proton-transfer motion, quenching tunneling, and originating in two different isotopologues determined by the deute-

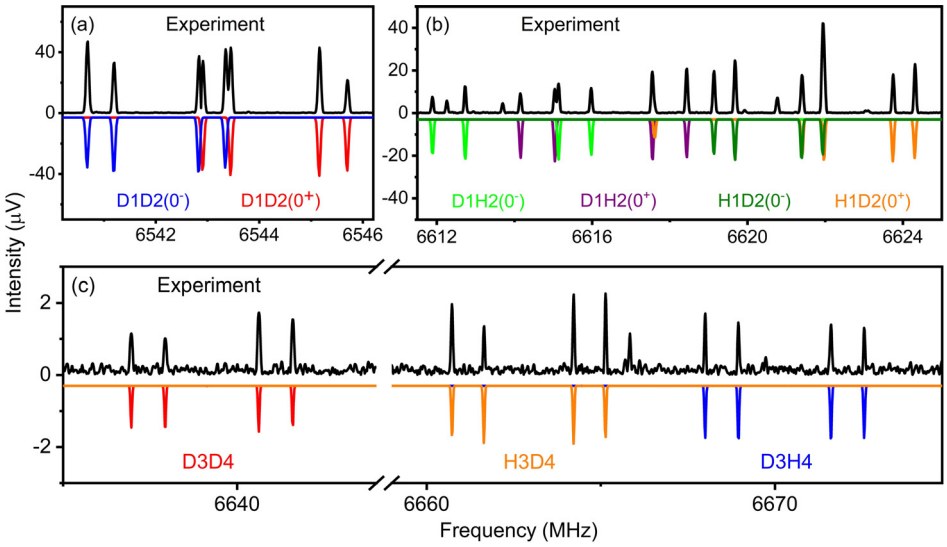

Figure 6. Parts of the rotational spectra of mono-deuterated and double-deuterated isotopologues. The quantum numbers of the quartet transitions are the same as for $J_{upper} = 6$ in Figure 2. The D1D2 spectrum is obtained from the signal average of 4.2 million measurements with the commercial DCOOH sample. The D1H2 and H1D2 spectra are resulting from 4.3 million FIDs with an 1:1 mixture of HCOOH and DCOOH. D3D4, H3D4, and D3H4 spectra are from a 4.5 million FIDs average with a mixture of samples FA and D_2O.

Table 3: Theoretical (ΔE_{01}^{theor}) and experimental (ΔE_{01}^{exp}) tunneling splittings in the PhF-FAD symmetric isotopologues.[a]

	Parent	D3D4	^{13}C1	^{13}C2	^{13}C3	^{13}C4	D1D2	D1H2	H1D2
ΔE_{01}^{theor}	269	6	167	156	269	256	470	217	169
ΔE_{01}^{exp}	267.6080(13)	–		267.6080(13)[b]			275.7992(84)	274.0545(77)	269.2596(74)

[a] Theoretical values were computed using the PBEh-3c/MM approximation. The atomic numeration is consistent with Figure 1, all values are in MHz. [b] This value was kept fixed at the value of the parent isotopologue.

rium positions. Replacement of both hydrogen atoms with deuteriums in the hydrogen-bonded system will not destroy the permutation-inversion symmetry along the double proton transfer path. However, the heavier mass of the moving particles in the D3D4 compared to the parent isotopologue leads to a lower tunneling rate, which can be confirmed by our theoretical calculation (Table 3). This makes the tunneling splitting in D3D4 unresolvable with our CP-FTMW spectrometer COMPACT (resolvable within 25 kHz). A technique with higher resolution, such as cavity-FTMW spectroscopy, could be used to observe this double deuterium transfer, but this is beyond the scope of the current research.

The described computational framework was also applied to the PhF-FAD isotopologues (see Table 3). The predicted tunneling splittings are in a worse agreement with the experiment than for the parent isotopologue. This is probably an effect of the vibrational Born-Oppenheimer approximation breakdown that appears from replacement of the nuclei by their heavy analogs due to a reduced energy difference between the vibrational energy levels.[32] Nevertheless there is a trend that only the symmetric deuteration (D3D4) significantly lowers the tunneling splitting in PhF-FAD, while the other symmetric isotopic substitutions have a weaker impact on the proton transfer.

In conclusion, we have applied chirped-pulse Fourier transform microwave (CP-FTMW) spectroscopy to investigate the effect of neighboring molecules on the proton transfer in the fluorobenzene–formic acid dimer (PhF-FAD) cluster. The π–π stacked geometry has retained a possibility for formic acid (FA) molecules in the FAD to exchange protons. The measured tunneling splitting in the PhF-FAD complex (267.6080(13) MHz) is smaller than in pure FAD (341(3) MHz). The quantum-chemical calculations show that the reaction barrier is not affected by the PhF molecule, while the effect is caused by the FAD environment reorganization during the course of the reaction. This result suggests that in flexible and weakly influencing environments the proton transfer rate would be lowered.[33]

Conflict of Interest

The authors declare no conflict of interest.

Keywords: effective Hamiltonian · hydrogen bonds · proton transfer · quantum tunneling · rotational spectroscopy

[1] P.-O. Löwdin, *Rev. Mod. Phys.* **1963**, *35*, 724–732.
[2] M. R. Blomberg, P. E. Siegbahn, *Biochim. Biophys. Acta (BBA) Bioenergetics* **2006**, *1757*, 969–980.
[3] A. Migliore, N. F. Polizzi, M. J. Therien, D. N. Beratan, *Chem. Rev.* **2014**, *114*, 3381–3465.
[4] J. P. Hosler, S. Ferguson-Miller, D. A. Mills, *Annu. Rev. Biochem.* **2006**, *75*, 165–187.
[5] R. Srivastava, *Front. Chem.* **2019**, *7*, 536.
[6] P. Muller, *Pure Appl. Chem.* **1994**, *66*, 1077–1184.
[7] K. Szalewicz in *Encyclopedia of Physical Science and Technology*, 3rd Edition (Ed.: R. A. Meyers), Academic Press, New York, **2003**, pp. 505–538.
[8] S. Cukierman, *Biochim. Biophys. Acta (BBA) Bioenergetics* **2006**, *1757*, 876–885.
[9] A. D. Godbeer, J. S. Al-Khalili, P. D. Stevenson, *Phys. Chem. Chem. Phys.* **2015**, *17*, 13034–13044.
[10] E. G. Weidemann, G. Zundel, *Z. Naturforschung A* **1973**, *28*, 236–245.
[11] P. T. van Duijnen, B. T. Thole in *Environmental Effects on Proton Transfer. Ab Initio Calculations on Systems in a Semi-Classical, Polarizable Environment* (Eds.: R. Daudel, A. Pull-

man, L. Salem, A. Veillard), Springer Netherlands, Dordrecht, **1982**, pp. 85 – 95.
[12] A. Paasche, T. Schirmeister, B. Engels, *J. Chem. Theory Comput.* **2013**, *9*, 1765 – 1777.
[13] P. C. Gómez, L. F. Pacios, *Phys. Chem. Chem. Phys.* **2005**, *7*, 1374 – 1381.
[14] A. Domanskaya, K. Marushkevich, L. Khriachtchev, M. Räsänen, *J. Chem. Phys.* **2009**, *130*, 154509.
[15] S. Nishino, M. Nakata, *J. Phys. Chem. A* **2007**, *111*, 7041 – 7047.
[16] A. Gutiérrez-Quintanilla, M. Chevalier, R. Platakyte, J. Ceponkus, C. Crépin, *Phys. Chem. Chem. Phys.* **2020**, *22*, 6115 – 6121.
[17] A. Vdovin, J. Waluk, B. Dick, A. Slenczka, *ChemPhysChem* **2009**, *10*, 761 – 765.
[18] T. Wassermann, D. Luckhaus, S. Coussan, M. Suhm, *Phys. Chem. Chem. Phys.* **2006**, *8*, 2344 – 2348.
[19] M. Pietrzak, M. F. Shibl, M. Bröring, O. Kühn, H.-H. Limbach, *J. Am. Chem. Soc.* **2007**, *129*, 296 – 304.
[20] E. Jahr, G. Laude, J. O. Richardson, *J. Chem. Phys.* **2020**, *153*, 094101.
[21] K. Molčanov, B. Kojić-Prodić, *IUCrJ* **2019**, *6*, 156 – 166.
[22] H. V. L. Nguyen, I. Kleiner, *Phys. Sci. Rev.* **2020**, 20200037, https://doi.org/10.1515/psr-2020-0037.
[23] R. T. Saragi, M. Juanes, C. Pérez, P. Pinacho, D. S. Tikhonov, W. Caminati, M. Schnell, A. Lesarri, *J. Phys. Chem. Lett.* **2021**, *12*, 1367 – 1373.
[24] W. Li, L. Evangelisti, Q. Gou, W. Caminati, R. Meyer, *Angew. Chem. Int. Ed.* **2019**, *58*, 859 – 865; *Angew. Chem.* **2019**, *131*, 869 – 875.
[25] Y. Zhang, W. Li, W. Luo, Y. Zhu, C. Duan, *J. Chem. Phys.* **2017**, *146*, 244306.
[26] F. Kollipost, R. W. Larsen, A. V. Domanskaya, M. Nörenberg, M. A. Suhm, *J. Chem. Phys.* **2012**, *136*, 151101.
[27] R. A. Marcus, *Rev. Mod. Phys.* **1993**, *65*, 599 – 610.
[28] H. Azzouz, D. Borgis, *J. Chem. Phys.* **1993**, *98*, 7361 – 7374.
[29] P. M. Kiefer, J. T. Hynes, *J. Phys. Chem. A* **2002**, *106*, 1834 – 1849.
[30] P. M. Kiefer, J. T. Hynes, *J. Phys. Chem. A* **2002**, *106*, 1850 – 1861.
[31] H.-H. Limbach, K. B. Schowen, R. L. Schowen, *J. Phys. Org. Chem.* **2010**, *23*, 586 – 605.
[32] D. S. Tikhonov, *ChemRxiv* **2021**, https://doi.org/10.33774/chemrxiv-2021-v74sm-v3.
[33] The Supporting Information contains experimental parameters and linelists for all the isotopologues of PhF-FAD, experimental and theoretical structures of PhF-FAD, complete description of the MM force field parameterization procedure, figures depicting the double proton transfer Schrödinger equation parameters. All the theoretical calculations needed to reproduce the results given in this manuscript are available from a zip-archive. The in-house software used for calculations is available for download from the repository. D. S. Tikhonov, https://stash.desy.de/projects/MOLINC, **2020**.

Manuscript received: June 21, 2021
Revised manuscript received: August 6, 2021
Accepted manuscript online: August 27, 2021
Version of record online: October 15, 2021

